Reductive Coupling of Carbon Monoxide Ligands To Form Coordinated Bis(trimethylsiloxy)ethyne in Seven-Coordinate Niobium(I) and Tantalum(I) $[M(CO)_2(dmpe)_2Cl]$ Complexes†[1,2]

Patricia A. Bianconi, Raymond N. Vrtis, Ch. Pulla Rao, Ian D. Williams, Mary P. Engeler, and Stephen J. Lippard*

Department of Chemistry, Massachusetts Institute of Technology, Cambridge, Massachusetts 02139

Received April 16, 1987

A general procedure for the reductive coupling of carbonyl ligands in $[M(CO)_2(dmpe)_2Cl]$ complexes, M = Nb or Ta and dmpe = 1,2-bis(dimethylphosphino)ethane, is described. Reaction of $[M(CO)_2(dmpe)_2Cl]$ with 40% sodium amalgam in THF or glyme followed by filtration, addition of Me_3SiY, Y = Cl or CF_3SO_3 (triflate), and recrystallization from pentane produce $[M(Me_3SiOC{\equiv}COSiMe_3)(dmpe)_2Y]$ in 40–70% isolated yields. In an alternative route, the coupled ligand product could be obtained in 25% yield by using activated Mg dust and a group IV (4) metallocene dihalide, such as $(C_5Me_5)_2ZrCl_2$, in place of sodium amalgam. The molecular structures of four $[M(Me_3SiOC{\equiv}COSiMe_3)(dmpe)_2Y]$ molecules (M = Ta or Nb, Y = Cl; M = Ta, Y = CF_3SO_3 or $Cl_{0.8}I_{0.2}$) were determined by X-ray crystallography. The metrical parameters thus obtained, average C–C bond length, 1.32 (1) Å, M–C–O angle, 155.6 (7)°, and C–C–O angle, 132.8 (5)°, parallel those displayed by other complexes containing four-electron donating alkynes. The infrared and NMR spectral properties also support the formal assignment of the coupled ligand as bis(trimethylsiloxy)ethyne. Preliminary mechanistic studies of the reductive coupling reaction suggest that it proceeds through initial formation of the *cis*-$[M(CO)_2(dmpe)_2]^-$ anion, which can be silylated to form $[M(Me_3SiOCCOSiMe_3)(dmpe)_2Y]$.

Introduction

The formation of carbon–carbon bonds has long been a challenge to synthetic chemists. One such C–C bond making process that is both intellectually appealing and of potential practical value is to convert carbon monoxide into functionalized hydrocarbons by reaction chemistry in which the first step involves reductive coupling. Direct reduction of CO by alkali metals[3] or electrochemically[4] yields $M_2(C_2O_2)$ and higher oligomers, from which, upon further redox or solvolysis reactions, glycolic acid derivatives, ethylene glycol, oxalic acid, hexahydroxybenzene, and aci-reductone polymers have been isolated.[3-5] Reductive coupling of carbonyl ligands in soluble transition, lanthanide, or actinide metal complexes has also been achieved.[6] This approach affords better control of subsequent reaction products and stereochemistry. In the cases reported thus far, however, the oxygen atoms of the coupled ligand are coordinated to a metal atom.

In recent years we have been investigating the reductive coupling of alkyl isocyanide ligands in seven-coordinate complexes of the form $[M(CNR)_6X]^+$ (M = Mo or W; X = halide or cyanide)[7] and $[Mo(CNR)_4(bpy)Cl]^+$[2] (eq 1 and 2). Similar coupling reactions occur for Nb, Ta, and Mo

$$[M(CNR)_6X]^+ + Zn(s) \xrightarrow[H^+]{THF} [M(RHNCCNHR)(CNR)_4X]^+ \quad (1)$$

$$[Mo(CNR)_4(bpy)Cl]^+ + Zn(s) \xrightarrow[H^+]{THF} [Mo(RHNCCNHR)(CNR)_3(bpy)]^{2+} \quad (2)$$

complexes where, in the products, the coupled isocyanide ligand, formally the $RNCCNR^{2-}$ dianion, bridges two metal centers.[8] From these experimental studies and extended Hückel molecular orbital calculations[7f] we identified several factors that promote the isocyanide reductive coupling reaction. Specifically, eq 1 and 2 are favored by the high coordination numbers of the transition metals, the use of

† In this paper the periodic group notation in parentheses is in accord with recent actions by IUPAC and ACS nomenclature committees. A and B notation is eliminated because of wide confusion. Groups IA and IIA become groups 1 and 2. The d-transition elements comprise groups 3 through 12, and the p-block elements comprise groups 13–18. (Note that the former Roman number designation is preserved in the last digit of the new numbering: e.g., III → 3 and 13.)

(1) Part 24 of a continuing series on higher coordinate complexes. for part 23, see ref 2.

(2) Warner, S.; Lippard, S. J. *Organometallics* **1986**, *5*, 1716.

(3) (a) Liebig, J. *Ann. Chem. Pharm.* **1834**, *11*, 182. (b) Joannis, A. *C. R. Hebd. Seances Acad. Sci.* **1893**, *116*, 1518; **1914**, *158*, 874. (c) Pearson, T. G. *Nature (London)* **1933**, *131*, 166. (d) Hackspill, L.; van Altane, L A. *C. R. Hebd. Seances. Acad. Sci.* **1938**, *206*, 1818. (e) Scott, A. F. *Science (Washington, D.C.)* **1952**, *115*, 118. (f) Weiss, E.; Büchner, W. *Helv. Chim. Acta* **1963**, *46*, 1121; **1964**, *47*, 1415. (g) Büchner, W. *Helv. Chim. Acta* **1963**, *46*, 2111. (h) Weiss, E.; Büchner, W. *Z. Anorg. Allg. Chem.* **1964**, *330*, 251. (i) Weiss, E.; Büchner, W. *Chem. Ber.* **1965**, *98*, 126. (j) Ellis, J. E.; Fjare, K. L.; Hayes, T. G. *J. Am. Chem. Soc.* **1981**, *103*, 6100.

(4) (a) Silvestri, S.; Gambino, G.; Filardo, G.; Guainazzi, M.; Ercoli, R. *Gazz. Chim. Ital.* **1972**, *102*, 818. (b) Silvestri, S.; Gambino, G.; Filardo, G.; Spadaro, G.; Palmisano, L. *Electrochim. Acta* **1978**, *23*, 413. (c) Bockmair, G.; Fritz, H. P. *Z. Naturforsch., B: Anorg. Chem., Org. Chem.* **1975**, *30B*, 330. (d) Uribe, F. A.; Sharp, P. R.; Bard, A. J. *J. Electroanal. Chem.* **1983**, *152*, 173.

(5) (a) Büchner, W. *Helv. Chim. Acta* **1965**, *48*, 1229. (b) Barber, J. Ph.D. Thesis, Massachusetts Institute of Technology, 1981, Chapter III.

(6) (a) Manriquez, J. M.; McAlister, D. R.; Sanner, R. D.; Bercaw, J. E. *J. Am. Chem. Soc.* **1978**, *100*, 2716. (b) Wolczanski, P. T.; Bercaw, J. E. *Acc. Chem. Res.* **1980**, *13*, 121. (c) Berry, D. H.; Bercaw, J. E.; Jircitano, A. J.; Mertes, K. B. *J. Am. Chem. Soc.* **1982**, *104*, 4712. (d) Fagan, P. J.; Moloy, K. G.; Marks, T. J. *J. Am. Chem. Soc.* **1981**, *103*, 6959. (e) Katahira, D. A.; Moloy, K. G.; Marks, T. J. *Organometallics* **1982**, *1*, 1723. (f) Gambarotta, S.; Floriani, C.; Chiesi-Villa, A.; Guastini, C. *J. Am. Chem. Soc.* **1983**, *105*, 7295. (g) Evans, W. J.; Wayda, A. L.; Hunter, W. E.; Atwood, J. L. *J. Chem. Soc., Chem. Commun.* **1981**, 706. (h) Evans, W. J.; Grate, J. W.; Hughes, L. A.; Zhang, H.; Atwood, J. L. *J. Am. Chem. Soc.* **1985**, *107*, 3728. (i) Planalp, R. P.; Andersen, R. A. *J. Am. Chem. Soc.* **1983**, *105*, 7774. (j) Erker, G.; Czisch, P.; Schlund, R.; Angermund, K.; Krüger, C. *Angew. Chem., Int. Ed. Engl.* **1986**, *25*, 364. (k) Arnold, J.; Tilley, T. D. *J. Am. Chem. Soc.* **1985**, *107*, 6409.

(7) (a) Lam, C. T.; Corfield, P. W. R.; Lippard, S. J. *J. Am. Chem. Soc.* **1977**, *99*, 617. (b) Corfield, P. W. R.; Baltusis, L. M.; Lippard, S. J. *Inorg. Chem.* **1981**, *20*, 922. (c) Dewan, J. C.; Giandomenico, C. M.; Lippard, S. J. *Inorg. Chem.* **1981**, *20*, 4069. (d) Giandomenico, C. M.; Lam, C. T.; Lippard, S. J. *J. Am. Chem. Soc.* **1982**, *104*, 1263. (e) Caravana, C.; Giandomenico, C. M.; Lippard, S. J. *Inorg. Chem.* **1982**, *21*, 1860. (f) Hoffmann, R.; Wilker, C. N.; Lippard, S. J.; Templeton, J. L.; Brower, D. J. *J. Am. Chem. Soc.* **1983**, *105*, 146.

(8) (a) Cotton, F. A.; Roth, W. J. *J. Am. Chem. Soc.* **1983**, *105*, 3734. (b) Cotton, F. A.; Duraj, S. A.; Roth, W. J. *J. Am. Chem. Soc.* **1984**, *106*, 6987. (c) Lenz, D.; Brüddgam, I.; Hartl, H. *Angew. Chem., Int. Ed. Engl.* **1984**, *23*, 525.

0276-7333/87/2306-1968$01.50/0

linear or chelating ligands, proper orbital alignment during the coupling step, an electron-rich metal center and the need for a Lewis acid to bind the heteroatoms of the coupled ligand. Using these factors as a guideline, we searched for, and eventually identified, a system in which reductive coupling of two carbon monoxide ligands in the known[9] seven-coordinate $[M(CO)_2(dmpe)_2Cl]$ complexes, M = Nb or Ta and dmpe = 1,2-bis(dimethylphosphino)-ethane, was achieved (eq 3). Here we report the details

$$[M(CO)_2(dmpe)_2Cl] \xrightarrow[\text{Lewis acid}]{\text{reductant}} \xrightarrow{Me_3SiY} [M(Me_3SiOCCOSiMe_3)(dmpe)_2Y] \quad (3)$$

of this chemistry, including a much superior synthesis to that previously communicated by us[10] and the crystal structures of four of these reductively coupled products: M = Nb, Y = Cl (1); M = Ta, Y = Cl (2); M = Ta, Y = 0.8Cl and 0.2I (3); and M = Ta, Y = O_3SCF_3 (4). Preliminary studies that reveal aspects of the mechanism of eq 3 are also described.

Experimental Section

Materials. All reactions and manipulations were carried out under nitrogen, using standard Schlenk techniques or a Vacuum Atmospheres drybox. Solvents were distilled under nitrogen from sodium benzophenone ketyl and stored over molecular sieves. Deuteriated benzene was dried by passage through a column of alumina and stored over 3-Å molecular sieves. $[Nb(dmpe)_2(CO)_2Cl]$ (5) and $[Ta(dmpe)_2(CO)_2Cl]$ (6) were synthesized by using modified[11] literature procedures.[9] Forty percent sodium amalgam was prepared by a literature method.[12] Chlorotrimethylsilane (Me_3SiCl) (Aldrich, Petrarch), trimethylsilyl trifluoromethanesulfonate ($Me_3SiOSO_2CF_3$) (Aldrich), magnesium (J.T. Baker), and $[(C_5Me_5)_2ZrCl_2]$ (Strem) were obtained from commercial sources and used without further purification. $[(C_5Me_5)_2Zr(N_2)]_2(N_2)$ was kindly provided by Prof. J. A. Bercaw. Tetraethylammonium chloride (Et_4NCl) and tetra-*n*-hexylammonium chloride ($[(C_6H_{13})_4NCl]$ salts (Aldrich) were dried by heating them at 100 °C under vacuum for 5–6 days.

Preparation of $[Nb(Me_3SiOCCOSiMe_3)(dmpe)_2Cl]$ (1). A mixture containing $[Nb(dmpe)_2(CO)_2Cl]$ (5) (0.1179 g, 0.243 mmol), 40% sodium amalgam (0.958 g), and 6 mL of THF was stirred in a 25-mL flask for 24 h, during which time the color changed from orange to red-brown. The IR spectrum of the filtered solution displayed three CO stretching bands at 1750, 1670, and 1600 cm^{-1}. Addition of 0.090 mL of Me_3SiCl (0.71 mmol) to the filtered solution produced an immediate color change from red-brown to plum-red. After an additional 3 h of stirring, the color of the reaction mixture turned to dark green and the THF was removed in vacuo. The green product was then extracted into pentane which, upon cooling to −30 °C, yielded 0.103 g (67%) of crystalline $[Nb(Me_3SiOCCOSiMe_3)(dmpe)_2Cl]$ (1): IR (KBr pellet) 2958 (w), 2896 (m), 2800 (w), 1557 (m), 1421 (w), 1292 (w), 1277 (w), 1258 (sh), 1246 (m), 1140 (m), 1003 (m), 939 (s), 924 (sh), 890 (s), 846 (s), 758 (w), 725 (m), 694 (m), 628 (m), 594 (w), 450 (w) cm^{-1}; UV–vis (THF, 1.41 mM) 322 nm (11 000 M^{-1} cm^{-1}), 448 (sh), 641 (90). Anal. Calcd for $C_{20}H_{50}ClO_2P_4Si_2Nb$: C, 38.07; H, 7.99; Cl, 5.62. Found: C, 38.04; H, 8.07; Cl, 5.66.

Preparation of $[Ta(Me_3SiOCCOSiMe_3)(dmpe)_2Cl]$ (2) (Method A). A mixture of $[Ta(CO)_2(dmpe)_2Cl]$ (6) (0.114 g, 0.199 mmol), 40% sodium amalgam (0.65 g), and 5 mL of THF was stirred in a 25-mL flask for 8 h, during which time the solution changed its color from orange to red-brown. The IR spectrum of the solution phase of this mixture consisted of three CO stretching bands at 1740, 1675, and 1600 cm^{-1}. To the filtered mixture were added Me_3SiCl (0.065 mL, 0.512 mmol) and Et_4NCl (0.034 g, 0.205 mmol), resulting in an immediate color change from red-brown to plum-red. After an additional 5 h of stirring, the color of the solution became dark green. The THF solvent was removed in vacuo and the green product extracted into 4 mL of pentane which, upon cooling to −30 °C, yielded 0.096 g (67%) of $[Ta(Me_3SiOCCOSiMe_3)(dmpe)_2Cl]$ (2): $^{31}P\{^1H\}$ NMR (36.6 MHz, pentane) δ 24 (s); IR (KBr pellet) 2959 (w), 2897 (m), 2800 (w), 1547 (m), 1420 (w), 1290 (w), 1277 (w), 1258 (sh), 1248 (m), 1144 (m), 1015 (m), 938 (s), 924 (sh), 899 (m), 845 (s), 756 (w), 727 (m), 692 (w), 625 (w) cm^{-1}; UV–vis (THF, 1.341 × 10^{-4} M) 329 nm (12 400 M^{-1} cm^{-1}), 438 (sh), 580 (109). Anal. Calcd for $C_{20}H_{50}ClO_2P_4Si_2Ta$: C, 33.41; H, 7.01; Cl, 4.93. Found: C, 33.10; H, 6.40; Cl, 5.00.

This reaction was subsequently reproduced without the addition of Et_4NCl.

Reaction of $[Ta(CO)_2(dmpe)_2Cl]$ (6) with Mg, $HgCl_2$, $[(C_5Me_5)_2ZrCl_2]$, and Me_3SiCl To Form $[Ta(Me_3SiOCCOSiMe_3)(dmpe)_2Cl]$ (2) (Method B). Mg dust (1.0 g, 41 mmol) and $HgCl_2$ (1.37 g, 5 mmol) were stirred in 30 mL of THF and warmed slightly above room temperature for 5–10 min. After the addition of $[Ta(CO)_2(dmpe)_2Cl]$ (6) (0.573 g, 1 mmol) and $[(C_5Me_5)_2ZrCl_2]$ (0.432 g, 1 mmol), the reaction mixture was stirred at room temperature and monitored by solution IR. After a 3–12-h period of stirring, the CO stretching vibrational bands of 6 completely disappeared and new bands at 1710, 1600, and 1525 cm^{-1} grew in. The reaction mixture was filtered, and the filtrate was treated with Me_3SiCl (0.254 mL, 2 mmol) at −78 °C. The solution turned green upon warming to room temperature and stirring for 12 h. Removal of the solvent in vacuo, extraction of the residue with 40 mL of pentane, filtration, reduction of the volume of the filtrate to 4 mL, and cooling to −20 °C resulted in the formation of 0.18 g (25%) of $[Ta(Me_3SiOCCOSiMe_3)(dmpe)_2Cl]$ (2): ^1H NMR (250 MHz, C_6D_6) δ 1.51, 1.47 (s, PCH_3), 0.24 (s, $SiCH_3$); $^{13}C\{^1H\}$ NMR (67.9 MHz, C_6D_6) δ 2.20 ($SiMe_3$), 18.4, 19.5 (PCH_3), 33.6 (t, J_{C-P} = 8 Hz, PCH_2), 212.5 (quintet, J_{C-P} = 15 Hz, $\equiv COSiMe_3$); $^{31}P\{^1H\}$ NMR (THF) δ 25.0 (s); IR (Nujol mull) 1540 (m), 1420 (m), 1298 (w), 1280 (w), 1260 (sh), 1250 (s), 1145 (s, br), 1110 (m), 1020 (s), 945 (s), 930 (s), 910 (m, br), 850 (s), 760 (w), 730 (m), 700 (m), 630 (m) cm^{-1}. Anal. Calcd for $C_{20}H_{50}ClO_2P_4Si_2Ta$: C, 33.41; H, 7.01; Cl, 4.93. Found: C, 32.7; H, 6.63; Cl, 4.63.

Reaction of $[Ta(CO)_2(dmpe)_2Cl]$ (6) with Mg, I_2, $[(C_5Me_5)_2ZrCl_2]$, and Me_3SiCl To Form $[Ta(Me_3SiOCCOSiMe_3)(dmpe)_2Cl_{0.8}I_{0.2}]$ (3). Mg dust (1 g, 41 mmol) and I_2 (50–80 mg, 0.20–32 mmol) were stirred and warmed slightly above room temperature in 30 mL of THF until the solution was colorless (about 5 min). Compound 6 (0.573 g, 1 mmol) and $[(C_5Me_5)_2ZrCl_2]$ (0.432 g, 1 mmol) were added. The reaction workup procedure, carried out as described in the previous case, using Me_3SiCl (0.254 mL, 2 mmol) resulted in green crystals (0.366 g). This product was found to be a mixture of two compounds, based on solution spectroscopic data. These products could not be separated by fractional crystallization from pentane, methylene chloride, benzene, toluene, ether, or mixtures thereof; they decomposed when chromatographed on alumina or silica gel. They could not be distinguished by their crystal habits. Spectroscopic data for the mixture: ^1H NMR (C_6D_6) δ 1.78, 1.51, 1.49, 1.47 (s, PCH_3), 0.24, 0.22 (s, $SiCH_3$); $^{13}C\{^1H\}$ NMR (C_6D_6) δ 2.20 (s, $SiCH_3$), 11.7 (br, m, $SiCH_3$), 24.5, 19.5, 18.4, 17.8 (s, br, PCH_3), 34.9, 33.6 (t, $^2J_{C-P}$ = 9 Hz, PCH_2), 212.5, 211.6 (quintet, $^2J_{C-P}$ = 15 Hz, $\equiv COSiMe_3$); $^{31}P\{^1H\}$ NMR (THF) δ 14.0, 25.0; IR (Nujol mull) 1540 cm^{-1}.

Preparation of $[Ta(Me_3SiOCCOSiMe_3)(dmpe)_2(OSO_2CF_3)]$ (4). A mixture of 6 (0.11 g, 0.192 mmol), 40% sodium amalgam (0.714 g), and 6 mL of 1,2-dimethoxyethane (glyme) was stirred in a 25-mL round-bottomed flask for 12 h, during which time the color changed from orange-yellow to red-brown. The IR spectrum of the solution component of this mixture showed three CO stretching bands at 1740, 1675, and 1600 cm^{-1}. The mixture was then filtered, and to the filtrate was added 0.090 mL (0.466 mmol) of $Me_3SiOSO_2CF_3$. The solution immediately turned to green but was allowed to stir for an additional period of 5 h. The glyme was then removed in vacuo and the green product extracted into 4 mL of pentane which, upon cooling to −30 °C, yielded 0.0629 g (39%) of $[Ta(Me_3SiOCCOSiMe_3)(dmpe)_2$-

(9) Datta, S.; Wreford, S. S. *Inorg. Chem.* **1977**, *16*, 1134.
(10) Bianconi, P. A.; Williams, I. D.; Engeler, M. P.; Lippard, S. J. *J. Am. Chem. Soc.* **1986**, *108*, 311.
(11) (a) Bianconi, P. A. Ph.D. Thesis, Massachusetts Institute of Technology, 1986. (b) Bianconi, P. A.; Williams, I. D.; Lippard, S. J., to be submitted for publication.
(12) Fieser, L. F.; Fieser, M. In *Reagents for Organic Synthesis*; Wiley: New York, 1967; Vol. 1, p 1033.

Table I. Experimental Details[a,b] of the X-ray Diffraction Studies of [Nb(Me$_3$SiOCCOSiMe$_3$)(dmpe)$_2$Cl] (1), [Ta(Me$_3$SiOCCOSiMe$_3$)(dmpe)$_2$Cl] (2), [Ta(Me$_3$SiOCCOSiMe$_3$)(dmpe)$_2$Cl$_{0.8}$I$_{0.2}$] (3), and [Ta(Me$_3$SiOCCOSiMe$_3$)(dmpe)$_2$(OSO$_2$CF$_3$)] (4)

	1	2	3	4
formula	$C_{20}H_{50}ClO_2P_4Si_2Nb$	$C_{20}H_{50}ClO_2P_4Si_2Ta$	$C_{20}H_{50}Cl_{0.8}I_{0.2}O_2P_4Si_2Ta$	$C_{21}H_{50}F_3O_5P_4SSi_2Ta$
a, Å	16.486 (2)	16.432 (3)	16.399 (2)	16.381 (3)
b, Å	10.857 (2)	10.864 (3)	10.945 (2)	12.389 (2)
c, Å	19.274 (2)	19.224 (8)	19.209 (5)	18.626 (2)
β, deg	106.43 (1)	106.40 (2)	106.51 (1)	103.60 (2)
V, Å^3	3309	3292	3306	3674
fw	631.05	719.09	737.38	832.7
Z	4	4	4	4
ρ_{calcd},[c] g cm^{-3}	1.267	1.451	1.481	1.505
space group	$I2/a$	$I2/a$	$I2/a$	$P2_1/c$
radiatn[d]		Mo Kα (0.710 69) Å		Cu Kα (1.5418 Å)
data limits, deg	$3 \le 2\theta \le 54$	$3 \le 2\theta \le 57$	$3 \le 2\theta \le 45$	$4 \le 2\theta \le 112$
cryst dimens, mm	0.375 × 0.3 × 0.2	0.375 × 0.25 × 0.125	0.20 × 0.30 × 0.54	0.4 × 0.325 × 0.2
linear abs coeff,[e] cm^{-1}	6.48	35.25	35.04	82.57
no. of data collected	3617	4158	3244	4776
no. of unique data[f]	2437	2933	2350	3024
no. of parameters refined	139	139	144	336
R_1[g]	0.0361	0.0370	0.0262	0.0472
R_2[h]	0.0507	0.0472	0.0351	0.0557

[a] Data were collected by $\theta/2\theta$ scans on an Enraf-Nonius CAD-4F κ-geometry diffractometer at 23 ± 1 °C. [b] Calculations were performed on a DEC VAX 11/780 computer using SHELX-76. [c] Since the crystals decompose, their densities could not be measured. [d] In case of Cu radiation, no monochromator was used. [e] Absorption corrections were performed either empirically from psi scans or with the Wehe–Busing–Levy ORABS program. [f] $I \ge 3\sigma(I)$ was used. [g] $R_1 = \sum||F_o| - |F_c||/\sum|F_o|$. [h] $R_2 = [\sum w||F_o| - |F_c||^2/\sum w|F_o|^2]^{1/2}$.

(OSO$_2$CF$_3$)] (**4**): ^{31}P{^{1}H} NMR (pentane) δ 28.8 (s); ^{19}F NMR (pentane) δ −77.8 (s); IR (KBr pellet) 2966 (w), 2898 (m), 2805 (m), 1575 (br, m), 1419 (m), 1316 (s), 1248 (s), 1233 (s), 1206 (s), 1180 (s), 1146 (s), 1031 (sh), 1013 (s), 935 (s), 900 (m), 847 (s), 788 (m), 755 (m), 698 (m), 629 (s), 582 (w), 518 (w), 507 (w), 450 (w) cm^{-1}; UV–vis (THF, 1.33 mM) 328 nm (ϵ 12 000 M^{-1} cm^{-1}), 458 (sh), 608 (160). Anal. Calcd for $C_{21}H_{50}F_3O_5P_4SSi_2Ta$: C, 30.29; H, 6.05; S, 3.85. Found: C, 29.95; H, 6.16; S, 3.83.

Spectral Measurements. ^{1}H and ^{13}C NMR spectra were recorded on Bruker WM-250 and WM-270 MHz instruments. ^{31}P NMR spectra were measured on a JEOL-FX 90 spectrometer and referenced to external 85% H_3PO_4. The ^{19}F NMR spectrum was obtained on the same instrument, using fluorobenzene (δ −113.1) as an internal standard; the reported ^{19}F chemical shifts are referenced to $CFCl_3$. Infrared spectra were recorded on a Beckman Acculab 10 grating or IBM IR/30S FTIR spectrometer. Electronic spectra were measured in the region 250–800 nm on a Perkin-Elmer Lambda 7 UV–visible spectrophotometer. Elemental analyses were performed by Galbraith Laboratories, Knoxville, TN.

Collection and Reduction of X-ray Data. [Nb(Me$_3$SiOCCOSiMe$_3$)(dmpe)$_2$Cl] (1). Green parallelepipeds were obtained directly by slow evaporation of the pentane extract of the reaction mixture (see above) at −30 °C. Since these crystals were large compared to the size required for X-ray purposes and were also extremely air-sensitive, they were reduced in volume by appropriate procedures,[13] mounted in 0.5-mm Lindemann glass capillaries with a protective coating of a thin layer of light element Apiezon grease, and studied on the diffractometer. The crystal used for data collection showed acceptable mosaic spread and no fine structure as checked through the open counter ω-scans of several strong, low-angle reflections ($\Delta\bar{\omega}_{1/2}$ = 0.19°). The Laue symmetry ($2/m$) and the systematic absences (hkl, $h + k + l \ne 2n$; $h0l$, h, $l \ne 2n$) revealed a body centered monoclinic lattice consistent with either a centrosymmetric, $I2/a$ (nonstandard setting of $C2/c$, No. 15), or a noncentrosymmetric, Ia (nonstandard setting of Cc, No. 9), space group.[14a] The subsequent successful determination and refinement of the structure indicated the centrosymmetric space group to be the correct one. Since there were no well-defined faces for the crystal used for data collection, an empirical absorption correction was applied. Further experimental details of data collection and reduction are presented in Table I.

[Ta(Me$_3$SiOCCOSiMe$_3$)(dmpe)$_2$Cl] (2). Red-green crystals of **2** were grown and mounted as described for **1**. A crystal with acceptable ω-scans was used for data collection and found to be isomorphous with **1**. The structure determination and refinement were carried out in space group $I2/a$. Since three intensity standard reflections measured after every 1 h of exposure showed 13% decay over the course of data collection, a linearly interpolated falloff correction was applied. Absorption corrections were made as described for **1**. Experimental details are presented in Table I.

[Ta(Me$_3$SiOCCOSiMe$_3$)(dmpe)$_2$Cl$_{0.8}$I$_{0.2}$] (3). This compound was obtained from a reaction where I_2 was used to activate magnesium as described above. Crystals were grown as described for **1** and mounted in capillaries. Data collected on an acceptable crystal showed **3** to be isomorphous with **1** and **2**. Intensity standards decayed by 37% linearly with time during the collection of data, which were corrected accordingly. An analytical absorption correction was applied. Experimental details of data collection and reduction are presented in Table I.

[Ta(Me$_3$SiOCCOSiMe$_3$)(dmpe)$_2$(OSO$_2$CF$_3$)] (4). Red-green crystals were grown by slow evaporation of a pentane extract of the reaction residue at −30 °C. Selection, manipulation, and handling of the crystals were as described for **1**. The crystals exhibited acceptable diffraction quality ($\Delta\bar{\omega}_{1/2}$ = 0.15–0.20°) with no fine structure. Study on the diffractometer revealed $2/m$ Laue symmetry and systematic absences ($h0l$, $l \ne 2n$; $0k0$, $k \ne 2n$), consistent with space group $P2_1/c$ (C_{2h}^5 No. 14).[14b] A linear falloff correction was applied to compensate for the observed 14% decay of standard reflections during data collection. Further details of the data collection and reduction are given in Table I.

Structure Determination and Refinement. Calculations were carried out by using the SHELX-76 program package.[15]

[Nb(Me$_3$SiOCCOSiMe$_3$)(dmpe)$_2$Cl] (1). An internal consistency index, R_{av},[16] was computed to be 2.1% based on 788 symmetry-related, low-angle, ($2\theta < 30°$) reflectons (h,$-k$, $\pm l$). The heavy-atom position derived from a Patterson map was confirmed through direct methods in centrosymmetric space group $I2/a$. Remaining non-hydrogen atoms were located from successive cycles of least-squares refinement, followed by difference Fourier syntheses. Both niobium and chlorine atoms sit on a twofold symmetry axis passing through the molecule. Eleven hydrogen atoms were recovered from difference Fourier maps, and the rest

(13) Rao, Ch. P., unpublished results.
(14) Hahn, T., Ed. *International Tables for Crystallography*; D. Reidel: Dordrecht, 1983: (a) pp 140, 182; (b) p 174.
(15) SHELX-76, a package of crystallographic programs written by G. M. Sheldrick. All computations were made on a DEC VAX 11/780 computer.
(16) Silverman, L. D.; Dewan, J. C.; Giandomenico, C. M.; Lippard, S. J. *Inorg. Chem.* **1980**, *19*, 3379.

Table II. Non-Hydrogen Atomic Coordinates for Compounds 1, 2, and 3[a]

	1, M = Nb			2, M = Ta			3, M = Ta[b]		
atom	*x*	*y*	*z*	*x*	*y*	*z*	*x*	*y*	*z*
M	0.2500	0.21771 (4)	0.0000	0.2500	0.21713 (3)	0.0000	0.2500	0.21798 (2)	0.0000
Cl	0.2500	0.45495 (12)	0.0000	0.2500	0.4539 (2)	0.0000	0.2500	0.4531 (8)	0.0000
P1	0.37600 (7)	0.26601 (10)	0.11049 (6)	0.37554 (12)	0.26788 (17)	0.10983 (9)	0.37625 (10)	0.26776 (13)	0.10980 (8)
P2	0.37285 (8)	0.25066 (10)	−0.05562 (7)	0.37182 (13)	0.24985 (18)	−0.05584 (11)	0.37193 (10)	0.25028 (14)	−0.05576 (9)
Si	0.29689 (8)	−0.15437 (10)	0.12607 (6)	0.29811 (12)	−0.15443 (18)	0.12616 (9)	0.29797 (10)	−0.15115 (14)	0.12634 (7)
O	0.32768 (15)	−0.0565 (2)	0.07334 (13)	0.3279 (2)	−0.0571 (4)	0.0725 (2)	0.3280 (2)	−0.0551 (3)	0.07328 (18)
C	0.2799 (2)	0.0365 (3)	0.03076 (17)	0.2815 (3)	0.0372 (5)	0.0310 (3)	0.2811 (3)	0.0392 (4)	0.0305 (2)
C1	0.1962 (3)	−0.2283 (4)	0.0802 (3)	0.1969 (5)	−0.2319 (7)	0.0808 (5)	0.1951 (4)	−0.2256 (6)	0.0808 (4)
C2	0.3836 (4)	−0.2676 (5)	0.1505 (4)	0.3851 (6)	−0.2690 (9)	0.1484 (6)	0.3832 (5)	−0.2659 (8)	0.1483 (5)
C3	0.2862 (5)	−0.0765 (7)	0.2077 (3)	0.2901 (8)	−0.0763 (12)	0.2098 (5)	0.2917 (7)	−0.0743 (11)	0.2115 (4)
C11	0.3671 (5)	0.3777 (7)	0.1794 (3)	0.3694 (6)	0.3755 (12)	0.1795 (5)	0.3717 (6)	0.3742 (9)	0.1818 (4)
C12	0.4375 (4)	0.1458 (6)	0.1662 (4)	0.4369 (6)	0.1447 (10)	0.1656 (6)	0.4385 (6)	0.1434 (9)	0.1632 (6)
C13	0.4581 (5)	0.3390 (9)	0.0786 (4)	0.4563 (7)	0.3489 (16)	0.0796 (6)	0.4586 (6)	0.3479 (14)	0.0787 (5)
C21	0.3679 (4)	0.3613 (6)	−0.1272 (3)	0.3652 (6)	0.3551 (11)	−0.1304 (5)	0.3661 (6)	0.3478 (10)	−0.1312 (5)
C22	0.4148 (4)	0.1150 (5)	−0.0877 (4)	0.4130 (6)	0.1138 (9)	−0.0886 (6)	0.4127 (6)	0.1191 (8)	−0.0880 (6)
C23	0.4667 (4)	0.3085(8)	0.0118 (4)	0.4677 (6)	0.3082 (12)	0.0125 (6)	0.4684 (5)	0.3070 (10)	0.0116 (5)
I							0.2500	0.4826 (8)	0.0000

[a] Numbers in parentheses are errors in the last significant digit(s). See Figure 1 for atom-labeling scheme. [b] Site occupancy factors are 0.8 for Cl and 0.2 for I.

were fixed, based on the standard geometry [d(C–H) = 0.95 Å]. All were constrained to "ride" on carbon atoms to which they were attached. These hydrogen atoms were refined with two common isotropic thermal parameters, one for the methylene (U = 0.27 Å^2) and one for the methyl groups (U = 0.22 Å^2), respectively. Scattering factors used in this and other structural studies reported in this paper were for neutral atoms and, together with anomalous dispersion corrections for the non-hydrogen atoms, were taken from ref 17. Hydrogen atom scattering factors were as given in ref 18. In the final stages of least-squares refinement, all non-hydrogen atoms were refined anisotropically. The function minimized was $\sum w(|F_o| - |F_c|)^2$, where the weights $w = 0.9517[\sigma^2(F_o) + 0.0009(F_o)^2]^{-1}$. Final R factors are reported in Table I; the maximum shift/esd was 0.07. A final difference electron density map showed no significant electron density. One carbon atom, labeled C3, of the trimethylsilyl group showed large anisotropic thermal parameters, possibly due to some unresolved disorder. Final non-hydrogen atomic positional and thermal parameters are given in Tables II and S1 (supplementary material), respectively, final hydrogen atom positional parameters are reported in Table S2, and a listing of observed and calculated structure factors appears in Table S3.

[Ta(Me$_3$SiOCCOSiMe$_3$)(dmpe)$_2$Cl] (2). The internal consistency index, R_{av} = 2.0%, computed for 537 symmetry-related reflections (h, $-k$,±l) in the range of 3° < 2θ < 16° reflects the high quality of the data. The structure determination and refinement were analogous to that reported for the isostructural molecule 1. Hydrogen atoms were constrained to "ride" on the carbon atoms to which they were attached. As for 1, hydrogen atoms were refined with two common isotropic thermal parameters, one for each of the methylene (U = 0.33 Å^2) and methyl (U = 0.20 Å^2) groups, respectively. In the final refinement cycles, weights were set equal to $w = 1.3595[\sigma^2(F_o) + 0.001(F_o)^2]^{-1}$. R factors are given in Table I, and the maximum final shift/esd was 0.03. The final difference electron density map was featureless. Again, there was one carbon atom of the silyl group (C3) that refined with large anisotropic thermal parameters, but a set of disordered positions could not be resolved. Final non-hydrogen atomic positional and thermal parameters are given in Tables II and S1, respectively, final hydrogen atom positional parameters are in Table S2, and a listing of observed and calculated structure factors appears in Table S4.

[Ta(Me$_3$SiOCCOSiMe$_3$)(dmpe)$_2$Cl$_{0.8}$I$_{0.2}$] (3). The computed R_{av} based on 87 symmetry-equivalent (0, k,$-l$) reflections was 1.9%. The structure determination and refinement procedures were analogous to those described above for the isostructural compounds 1 and 2. Toward the end of the refinement, and after the structure of 1 and 2 were known, the rather long Ta–Cl distance (2.727 Å)[10] and a 2.6 e/Å^3 electron density peak found in the differences Fourier map near the chloride ion suggested that the crystal might be a mixed-halide derivative. Data had been collected on crystals grown from a reaction in which 0.24 mmol of I_2/mmol of 6 was used to activate the magnesium. It therefore seemed likely that there was a contamination of iodide in the compound, since replacement of Cl^- with I^- would not change the molecular geometry. Removal of the chlorine atom from the model and examination of a difference Fourier map revealed two peaks on the twofold symmetry axis just barely resolvable, ~0.39 Å apart. A model was thus introduced in which [Ta(Me$_3$SiOCCOSiMe$_3$)(dmpe)$_2$Y] molecules, Y = Cl$_x$ and I$_{1-x}$, were randomly distributed at the same sites throughout the crystal lattice. Refinement of the site occupancy factor proceeded smoothly to x = 0.8. The resulting Ta–Y bond lengths were in good agreement with the expected values, as discussed below. Moreover, the 4:1 Cl to I ratio is the same as the mole ratio of I_2 to [Ta(CO)$_2$(dmpe)$_2$Cl] (6) used in the coupling reaction. The final R factors thus obtained (R_1 = 2.62%, R_2 = 3.51%; see Table I) are substantially better than those (R_1 = 4.6%, R_2 = 4.4%) found for the original model. Hydrogen atoms were fixed as described for 2, and the common isotropic thermal parameters (U) for both methylene and methyl groups refined to 0.42 and 0.24 Å^2, respectively. The weighting scheme employed in final refinement cycles was $w = 1.018[\sigma^2(F_o) + 0.000\,625(F_o)^2]^{-1}$. The maximum final shift/esd was 0.026. A difference Fourier map computed after the fractional iodide contribution was introduced to the model was featureless. The C3 silyl group carbon atom of this structure also exhibited large anisotropic thermal parameters, as was the case for 1 and 2. Final non-hydrogen atomic positional and thermal parameters are given in Tables II and S1, respectively, final hydrogen atom positional parameters in Table S2, and a listing of observed and calculated structure factors in Table S5.

[Ta(Me$_3$SiOCCOSiMe$_3$)(dmpe)$_2$(OSO$_2$CF$_3$)] (4). The R_{av} value was 3.9% for 805 symmetry-related reflections (±h,±k,±l) collected in the range 4° < 2θ < 36°. The heavy atom was located from a Patterson map and the rest of the non-hydrogen atoms from difference Fourier maps and least-squares refinement cycles. Difference Fourier maps also yielded 39 hydrogen atoms, and the rest were calculated from the expected geometry and constrained to "ride" on carbon atoms to which they were attached. Common isotropic temperature factors (U) refined to 0.09 and 0.14 Å^2, respectively, for methylene and methyl hydrogen atoms. In the final refinement, weights were set to $0.9022[\sigma^2(F_o) + 0.0006(F_o)^2]^{-1}$. The final disagreement indices were as reported in Table I, and the maximum shift/esd was 0.007. A final difference Fourier map showed no appreciable residual electron density. Final non-hydrogen atomic positional and thermal parameters are given in

(17) *International Tables for X-ray Crystallography*; Kynoch: Birmingham, England, 1974; Vol. IV, pp 99, 149.
(18) Stewart, R. F.; Davidson, E. R.; Simpson, W. T. *J. Chem. Phys.* **1965**, *42*, 3175.
(19) Hoffmann, R.; Beier, B. F.; Muetterties, E. L.; Rossi, A. R. *Inorg. Chem.* **1977**, *16*, 511.

Table III. Non-Hydrogen Atomic Coordinates for Compound 4[a]

atom	x	y	z
Ta	0.22767 (3)	0.06843 (5)	0.76210 (3)
P1	0.08812 (19)	0.0458 (2)	0.66696 (18)
P2	0.19590 (19)	0.2608 (3)	0.71169 (17)
P3	0.3363 (2)	0.0775 (3)	0.88449 (17)
P4	0.2315 (2)	-0.1215 (3)	0.8117 (2)
OT1	0.1392 (5)	0.1048 (6)	0.8379 (4)
C1	0.3366 (7)	0.0381 (9)	0.7265 (7)
C2	0.2690 (7)	0.0339 (9)	0.6682 (6)
C11	-0.0095 (7)	0.0363 (10)	0.6992 (7)
C12	0.0721 (8)	-0.0686 (10)	0.6005 (7)
C13	0.0662 (8)	0.1661 (10)	0.6069 (7)
C21	0.2020 (8)	0.3869 (10)	0.7657 (7)
C22	0.2544 (7)	0.2950 (10)	0.6449 (6)
C23	0.0877 (7)	0.2676 (9)	0.6536 (6)
C31	0.4254 (8)	0.1727 (12)	0.9031 (7)
C32	0.3049 (9)	0.0910 (13)	0.9698 (7)
C33	0.3885 (9)	-0.0545 (12)	0.8983 (8)
C41	0.1440 (8)	-0.1791 (12)	0.8417 (8)
C42	0.2534 (10)	-0.2270 (12)	0.7476 (8)
C43	0.3195 (9)	-0.1435 (12)	0.8936 (8)
S	0.0955 (2)	0.1876 (3)	0.87022 (18)
OT2	0.0301 (6)	0.2389 (7)	0.8178 (5)
OT3	0.1488 (6)	0.2529 (7)	0.9237 (5)
CT	0.0390 (11)	0.1039 (13)	0.9228 (9)
F1	0.0926 (7)	0.0500 (7)	0.9752 (5)
F2	-0.0057 (6)	0.1654 (8)	0.9588 (5)
F3	-0.0116 (6)	0.0362 (7)	0.8823 (5)
O1	0.4189 (5)	0.0127 (7)	0.7292 (5)
O2	0.2504 (5)	0.0167 (8)	0.5934 (4)
Si1	0.5084 (2)	0.0727 (4)	0.7354 (2)
Si2	0.3040 (3)	-0.0241 (3)	0.5361 (2)
C3	0.5572 (9)	0.0055 (14)	0.6654 (9)
C4	0.5845 (9)	0.0448 (13)	0.8302 (9)
C5	0.4932 (8)	0.2238 (11)	0.7213 (8)
C6	0.3642 (10)	-0.1472 (11)	0.5726 (8)
C7	0.3710 (11)	0.0871 (12)	0.5145 (10)
C8	0.2257 (10)	-0.0502 (12)	0.4512 (7)

[a] Numbers in parentheses are errors in the last significant digit(s). See Figure 2 for atom labels.

Tables III and S6, respectively, final hydrogen atom positional parameters in Table S7, and a listing of observed and calculated structure factors in Table S8.

Results and Discussion

Syntheses and Preliminary Mechanistic Studies. Reductive coupling of two carbon monoxide ligands occurs when seven-coordinated niobium(I) and tantalum(I) complexes are reduced in the presence of a Lewis acid and subsequently treated with trimethylsilyl chloride or triflate (eq 3). The $[M(CO)_2(dmpe)_2Cl]$ complexes were identified as good candidates for promoting this reaction for several reasons. X-ray structural studies revealed close nonbonded contacts between the two carbonyl carbon atoms, situated on the unique edge of C_{2v}-capped trigonal prisms: $[Nb(CO)_2(dmpe)_2Cl]$, 2.30 (3), 2.29 (3) Å; $[Nb(CO)_2(dmpe)_2I]$, 2.24 (12) Å; $[Ta(CO)_2(dmpe)_2Me]$, 2.29 (2) Å; and C–M–C angles of 70° or less.[11,20] Calculations have shown that a small positive overlap population of 0.024 exists between the two ligands on the unique edge of a C_{2v}-capped trigonal prism, indicative of attractive interactions.[19] Such interactions may contribute to the propensity of alkyl isocyanide analogues, for example, $[Mo(CNR)_6I]^+$, to undergo reductive coupling.[7] In addition, the low carbonyl infrared stretching frequencies of 1810 and 1747 cm^{-1} for $[Nb(CO)_2(dmpe)_2Cl]$ (**5**) and 1833 and 1756 cm^{-1} for $[Ta(CO)_2(dmpe)_2Cl]$ (**6**) revealed their electron-rich character, another factor associated with the reductive coupling of analogous alkyl isocyanide complexes.[7e]

Two routes to the reductively coupled products have been discovered in this investigation. As shown in eq 3, a reducing agent is first added to a THF solution containing **6**. In one route (method B), the reducing agent is magnesium, activated by I_2 or $HgCl_2$, and is followed by addition of a metallocene dihalide as a Lewis acid. When the solution is stirred at room temperature for several hours, the color changes from yellow to red-brown and the CO stretching bands of **6** disappear and new bands at 1710, 1600, and 1525 cm^{-1} grow in. These bands were previously postulated to arise from species containing η^2-CO bridges between Ta and Zr when $[(C_5Me_5)_2ZrCl_2]$ was used as the Lewis acid,[10] but several attempts to isolate and structurally characterize this intermediate have proved futile. Moreover, we have subsequently been able to generate a very similar solution infrared spectrum by using magnesium anthracene and no metallocene dihalide as the reducing agent or by the $Mg/HgCl_2$ method at 45 °C with no added metallocene dihalide. Addition of trimethylsilyl chloride to these solutions yields **2**.[20] These results, together with information about the spectroscopic properties of the red-brown intermediate generated by method A described below, suggest that two of the low-frequency infrared bands result from reaction of $[Ta(CO)_2(dmpe)_2]^-$ with solvated Mg^{2+} ions to form an isocarbonyl in which magnesium, and not Zr(IV), is bonded to the oxygen atoms of the bridging carbonyl groups. In method B, the metallocene dihalides may facilitate electron transfer between magnesium and the tantalum complex **6**. An attempt to use the known complex $[(C_5Me_5)_2Zr(N_2)](N_2)$[21] directly as the reductant produced a deep purple-red solution which turned green over time without addition of Me_3SiCl. The infrared spectrum showed only the CO bands of the starting material **6**. Perhaps the addition of Mg^{2+} salts to this reaction would have effected formation of the desired red-brown intermediate, but this possibility was not investigated.

In the second route (method A), 40% sodium amalgam is used as both reductant and Lewis acid, the latter presumably being solvated Na^+ ions. This reaction occurs smoothly for both **5** and **6** and produces infrared spectral bands at 1750, 1670, and 1600 cm^{-1} for Nb and at 1740, 1675, and 1600 cm^{-1} for Ta. These bands appear to result from two different species since their relative intensities vary with time, the 1750 or 1740 cm^{-1} band first increasing and then diminishing as the reaction proceeds. The nature of this species is presently unknown. The two low-frequency infrared bands grow in continuously with increasing reaction time. They may be due to the two-electron reduction product *cis*-$[M(CO)_2(dmpe)_2]^-$, ion paired with Na^+ ions in solution. Addition of tetra-*n*-hexylammonium chloride to this solution led, in the case where M = Ta, to the formation of red-orange crystals of $[(n\text{-}C_6H_{13})_4N][Ta(CO)_2(dmpe)_2]$, the crystal structure of which contains *cis*-dicarbonylbis[(1,2-bis(dimethylphosphino)ethane]tantalum(-I) ion, as will be described elsewhere.[20] A Nujol mull infrared spectrum of this compound exhibited CO stretching bands at 1695 and 1600 cm^{-1}.

Once the red-brown solution containing the low-frequency carbonyl stretching bands is generated by either method A or B and filtered, addition of Me_3SiY, where $Y^- = Cl^-$ or $CF_3SO_3^-$, leads to the formation of the desired green, reductively coupled products. These compounds, which contain the coordinated η^2-$Me_3SiOCCOSiMe_3$ lig-

(20) Rao, Ch. P.; Vrtis, R. N.; Lippard, S. J., unpublished results.

(21) Manriquez, J. M.; McAlister, D. R.; Rosenberg, E.; Shiller, A. M.; Williamson, K. L.; Chan, S. I.; Bercaw, J. E. *J. Am. Chem. Soc.* **1978**, *100*, 3078.

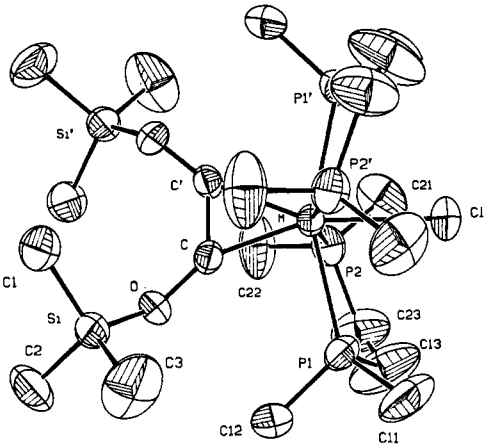

Figure 1. Generic structure of the isomorphous series of [M(Me$_3$SiOCCOSiMe$_3$)(dmpe)$_2$Y] complexes **1** (M = Nb, Y = Cl), **2** (M = Ta, Y = Cl), and **3** (M = Ta, Y = $Cl_{0.8}I_{0.2}$), showing the atom-labeling scheme and 40% thermal ellipsoids for **2**.

and, can be readily identified in solution by their characteristic infrared and ^{31}P NMR spectra (vide infra). If we consider the bis(trimethylsiloxy)ethyne ligand to be a four-electron donor, an assignment consistent with its molecular geometry and ^{13}C NMR spectrum,[22] the products **1–4** all achieve an 18-electron noble-gas configuration. A similar metal-bound trimethylsiloxy ligand occurs in [Fe_2(Me$_3$SiOC)$_4$(CO)$_6$].[23]

Since the ligand trans to the coordinated alkyne in **1–4** can be chloride or triflate, depending upon the choice of Y in Me$_3$SiY, or even iodide if I_2 is used to activate Mg in method B, it would appear that at some point during the reaction pathway the chloride ligand of the starting material **5** or **6** is either lost or labilized. Previous work has shown that the chloride capping ligand in **6** is kinetically inert, and only exchanges by reduction to the [Ta(CO)$_2$(dmpe)$_2$]$^-$ anion followed by oxidative addition of, for example, HX.[9] These observations further support the postulated role of such an anion in the reaction mechanism. Although we tentatively assigned spectroscopic features observed in a mixture of reaction products of eq 3 to the trimethylsilyl-capped analogue "[Ta(Me$_3$SiOCCOSiMe$_3$)(dmpe)$_2$(SiMe$_3$)]", the similarity of these spectral properties, especially the ^{31}P NMR spectrum, to those of the iodide-capped complex and the identification of this species as a contaminant in the structure of **3** suggest that the spectral features derive from the iodide-capped coupled ligand product.

Because of its greater simplicity and higher yields, method A is the preferred route to generate [M(R$_3$SiOCCOSiR$_3$)(dmpe)$_2$Y] complexes. Although the R groups were not varied in reactions by using this method, extensive studies using method B, in which the products were spectroscopically characterized, demonstrated that a variety of silyl halides may be employed. Specifically, coupled ligand products were observed for Me$_3$SiCl, Ph$_2$MeSiCl, PhMe$_2$SiCl, (*t*-Bu)Me$_2$SiCl, BzMe$_2$SiCl, and HMe$_2$SiCl but not for (*i*-Pr)$_3$SiCl, Et$_3$SiCl, or Ph$_3$SiCl. These results suggest that at least one sterically undemanding alkyl group, Me in all successful cases, is preferred, possibly for intramolecular packing reasons revealed by the structural studies of **1–4**.

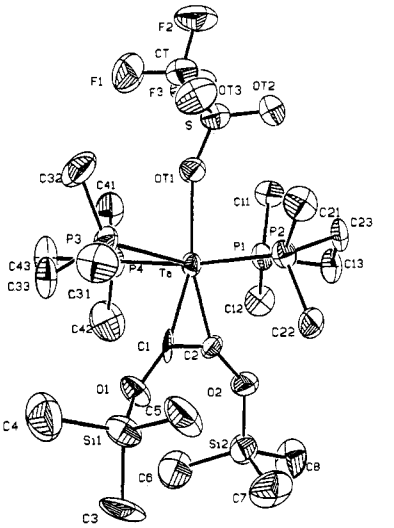

Figure 2. Structure of [Ta(Me$_3$SiOCCOSiMe$_3$)(dmpe)$_2$(OSO$_2$CF$_3$)] (**4**), showing the 40% thermal ellipsoids and atom-labeling scheme.

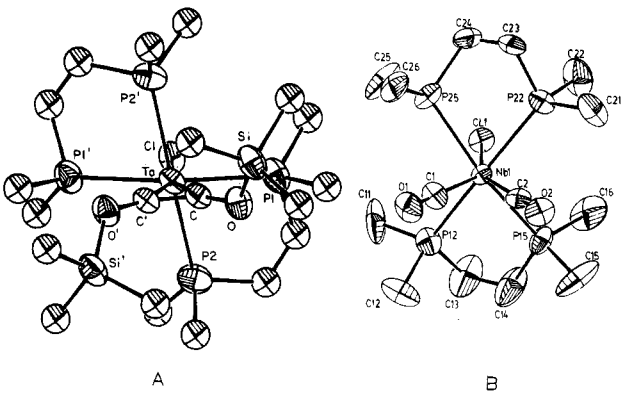

Figure 3. Comparison of the structures of (A) [Ta(Me$_3$SiOCCOSiMe$_3$)(dmpe)$_2$Cl] (**3**) and (B) [Nb(CO)$_2$(dmpe)$_2$Cl] (**5**) viewed approximately down the molecular C_2 axes.

Structures of [M(Me$_3$SiOCCOSiMe$_3$)(dmpe)$_2$Y] Complexes 1–4. The structure of [Ta(Me$_3$SiOCCOSiMe$_3$)(dmpe)$_2$Cl] (**2**) is shown in Figure 1. All three members of the isomorphous series of compounds **1–3** lie on a crystallographically required twofold symmetry axis that passes through the metal, halide, and midpoint of the C–C bond of the acetylene diether ligand. The triflate analogue **4** has a similar structure (Figure 2) but only C_1 point group symmetry. The coupled ligand and the halide or triflate anion are trans to one another in the coordination sphere, which is completed by two chelating 1,2-bis(dimethylphosphino)ethane ligands in the equatorial positions. Molecules **1–4** may thus be described as having either seven-coordinate geometries, analogous to those of [Mo(RHNCCNHR)(CNR)$_4$X]$^+$ cations,[7] or distorted octahedral structures, in which the midpoint of the –C≡C– bond is considered to occupy one of the six coordination positions. When viewed down the Ta–Y bond axis, it is apparent that the metal centers in **2** (Figure 3) and its analogues are chiral, a feature that could ultimately prove valuable in achieving the synthesis of optically active products by subsequent reaction chemistry of **1–4** and related molecules.

Selected bond lengths and angles for **1–4** are reported in Table IV. Table V compares metal–ligand bond distances and geometric features of the coordinated bis(trimethylsiloxy)ethyne moiety for **1–4** and some related molecules. The Ta–Cl and Ta–P bond distances are sim-

(22) (a) Cotton, F. A.; Hall, W. T. *J. Am. Chem. Soc.* **1979**, *101*, 5094. (b) Smith, G.; Schrock, R. R.; Churchill, M. R.; Youngs, W. J. *Inorg. Chem.* **1981**, *20*, 387. (c) Templeton, J. L.; Ward, B. C. *J. Am. Chem. Soc.* **1980**, *102*, 3288. (d) Curtis, M. D.; Real, J. *Organometallics* **1985**, *4*, 940.

(23) (a) Nasta, M. A.; MacDiarmid, A. G.; Saalfeld, F. E. *J. Am. Chem. Soc.* **1972**, *94*, 2449. (b) Bennett, M. J.; Graham, W. A. G.; Smith, R. A.; Stewart, R. P., Jr. *J. Am. Chem. Soc.* **1973**, *95*, 1684.

Table IV. Interatomic Distances (Å) and Angles (deg) for 1-4[a]

	M = Nb (1)	M = Ta (2)	M = Ta (3)		M = Nb (1)	M = Ta (2)	M = Ta (3)
Bond Lengths							
M–C	2.074 (3)	2.065 (5)	2.065 (4)	M–I			2.896 (9)
M–P1	2.573 (1)	2.561 (2)	2.559 (1)	C–C′	1.310(6)	1.339 (9)	1.316 (9)
M–P2	2.571 (2)	2.545 (2)	2.547 (2)	C–O	1.396 (4)	1.387 (6)	1.405 (5)
M–Cl	2.576 (1)	2.571 (2)	2.58 (1)	O–Si	1.647 (3)	1.642 (5)	1.634 (3)
Bond Angles							
C–M–P1	83.48 (9)	83.6 (1)	83.8 (1)	P1–M–P1′	156.48 (5)	155.16 (8)	155.42 (6)
C–M–P2	95.8 (1)	95.1 (2)	95.2 (1)	P2–M–P2′	164.00 (5)	163.95 (9)	164.04 (7)
C–M–Cl,I	161.58 (8)	161.1 (1)	161.4 (1)	P1–M–Cl,I	78.20 (3)	77.54 (4)	77.71 (3)
C–M–C′	36.8 (2)	37.8 (3)	37.2 (2)	P2–M–Cl,I	81.94 (3)	82.01 (4)	82.01 (4)
C′–M–P1	120.02 (9)	121.2 (1)	120.8 (1)	M–C–C′	71.6 (3)	71.1 (4)	71.5 (3)
C′–M–P2	99.4 (1)	100.0 (2)	99.9 (1)	M–C–O	154.6 (2)	156.4 (4)	155.7 (3)
P1–M–P2	76.72 (4)	76.75 (6)	76.7 (1)	C′–C–O	133.4 (2)	132.3 (3)	132.7 (2)
P1–M–P2′	99.99 (4)	99.76 (6)	99.89 (5)	C–O–Si	127.5 (2)	128.6 (4)	128.7 (3)

Compound 4

Bond Lengths										
Ta–C1	2.08 (1)	Ta–C2	2.06 (1)	Ta–P1	2.557 (3)	Ta–OT1	2.293 (8)	C1–C2	1.36 (1)	C1–O1	1.37 (1)
Ta–P2	2.571 (3)	Ta–P3	2.543 (3)	Ta–P4	2.524 (4)	C2–O2	1.37 (1)	O1–Si1	1.623 (9)	O2–Si2	1.62 (1)

Bond Angles								
C1–Ta–C2	38.3 (4)	C1–Ta–P1	117.0 (3)	P2–Ta–P3	109.1 (1)	P2–Ta–P4	169.8 (1)	
C1–Ta–P2	99.6 (3)	C1–Ta–P3	79.7 (3)	P3–Ta–P4	76.1 (1)	P1–Ta–OT1	81.8 (2)	
C1–Ta–P4	89.9 (3)	C1–Ta–OT1	161.0 (3)	P2–Ta–OT1	86.6 (2)	P3–Ta–OT1	81.4 (2)	
C2–Ta–P1	79.0 (3)	C2–Ta–P2	87.7 (3)	P4–Ta–OT1	85.5 (2)	Ta–C1–C2	70.2 (7)	
C2–Ta–P3	117.9 (3)	C2–Ta–P4	97.7 (3)	Ta–C2–C1	71.5 (7)	Ta–C1–O1	159.9 (9)	
C2–Ta–OT1	160.7 (3)	P1–Ta–P2	77.08 (9)	Ta–C2–O2	148.7 (9)	C2–C1–O1	129 (1)	
P1–Ta–P3	161.6 (1)	P1–Ta–P4	95.4 (1)	C1–C2–O2	140.0 (1)	C1–O1–Si1	139.5 (8)	
				C2–O2–Si2	134.0 (8)			

Intraligand Geometry[b]

compd	bond or angle type	min	max	mean	compd	bond or angle type	min	max	mean
1	Si–C	1.832 (5)	1.842 (6)	1.837 (6)	3				1.42 (1)
2		1.849 (8)	1.85 (1)	1.85 (1)	4		1.52 (2)	1.57 (2)	1.55 (2)
3		1.836 (8)	1.869 (8)	1.853 (8)	1	C–P–C	99 (2)	102.6 (3)	100.7 (3)
4		1.81 (1)	1.94 (1)	1.88 (1)	2		96.9 (6)	102.1 (5)	100.4 (6)
1	O–Si–C	103.6 (2)	112.4 (2)	108.9 (3)	3		97.7 (5)	101.9 (5)	100.0 (5)
2		103.3 (4)	112.6 (3)	108.9 (4)	4		98.8 (7)	103.6 (6)	101.3 (7)
3		103.8 (3)	112.5 (2)	109.1 (3)	1	C–C–P	117.2 (5)	119.7 (6)	118.5 (6)
4		104.4 (6)	111.1 (6)	108.7 (6)	2		116.0 (10)	116.4 (8)	116.2 (9)
1	C–Si–C	108.8 (3)	111.3 (2)	110.1 (3)	3		115.3 (7)	116.6 (6)	116.0 (7)
2		109.7 (4)	110.2 (5)	110.0 (5)	4		108.3 (9)	110.0 (10)	109.9 (7)
3		109.8 (4)	110.1 (4)	110.0 (4)	4	S–OT	1.414 (9)	1.459 (9)	1.431 (9)
4		105.5 (7)	113.8 (7)	110.1 (7)	4	S–CT			1.82 (2)
1	P–C	1.807 (6)	1.834 (7)	1.819 (7)	4	CT–F	1.29 (2)	1.34 (2)	1.32 (2)
2		1.80 (1)	1.86 (1)	1.82 (1)	4	OT–S–OT	113.3 (5)	118.0 (5)	115.2 (5)
3		1.768 (8)	1.846 (9)	1.816 (8)	4	OT–S–CT	100.5 (7)	104.8 (7)	102.9 (7)
4		1.79 (1)	1.86 (1)	1.84 (1)	4	F–CT–F	105.0 (10)	109.0 (10)	107.3 (10)
1	(P)C–C(P)			1.37 (1)	4	F–CT–S	110.0 (10)	113.0 (10)	111.3 (10)
2				1.42 (1)					

[a] See footnote *a* in Tables II and III. Primed and unprimed atoms are related by a twofold symmetry axis. [b] Standard deviations, quoted for mean values, are the average of the standard deviations for the individual values. Distances have not been corrected for thermal motion. T refers to the triflate group.

Table V. Selected Features of the Coordination and Coupled Ligand Geometry of Low-Valent M(dmpe)$_2$-Containing Complexes (M = Nb, Ta)[a]

complex	M–Cl	M–P	M–C(O)	(O)C–C(O)	C–M–C
$[Ta(dmpe)_2Cl_2]$[b]	2.427 (2)	2.519 (2)			
$[Ta(\eta^4\text{-}C_{10}H_8)(dmpe)_2Cl]$[c]	2.596 (1)	2.599 (15)			
$[Ta(\eta^4\text{-}C_{14}H_{10})(dmpe)_2Cl]$[b]	2.582 (3)	2.600 (3)			
$[Ta(dmpe)_2(CO)_2Cl]$ (6)[d]	2.62 (1)	2.58 (2)	1.98 (5)	2.28 (7)	70 (2)
$[Ta(dmpe)_2(CO)_2(OSO_2CF_3)]$[d]		2.578 (3)	1.97 (1)	2.14 (2)	66.0 (6)
$[Ta(dmpe)_2(CO)_2Me]$[d]		2.564 (2)	2.083 (8)	2.29 (2)	66.7 (4)
$[Nb(Me_3SiOCCOSiMe_3)(dmpe)_2Cl]$ (1)[e]	2.576 (1)	2.572 (2)	2.074 (3)	1.310 (6)	36.8 (2)
$[Ta(Me_3SiOCCOSiMe_3)(dmpe)_2Cl]$ (2)[e]	2.571 (2)	2.553 (2)	2.065 (5)	1.339 (9)	37.8 (3)
$[Ta(Me_3SiOCCOSiMe_3)(dmpe)_2Cl_{0.8}I_{0.2}]$ (3)[e]	2.58 (1)	2.553 (2)	2.065 (4)	1.316 (9)	37.2 (2)
$[Ta(Me_3SiOCCOSiMe_3)(dmpe)_2(OSO_2CF_3)]$ (4)[e]		2.549 (3)	2.07 (1)	1.36 (1)	38.3 (4)

[a] Bond lengths are given in Å and angles in deg. Numbers in parentheses are estimated standard deviations in the last digit(s) given. [b] Reference 11. [c] Reference 24. [d] Reference 20. [e] This work.

ilar to those found in the $[Ta(CO)_2(dmpe)_2Y]$ starting materials,[11] in $[Ta(\eta^4\text{-anthracene})(dmpe)_2Cl]$,[11] and in $[Ta(\eta^4\text{-naphthalene})(dmpe)_2Cl]$[24] but are longer than the values found in the lower coordinate, higher oxidation state

molecule $[Ta(dmpe)_2Cl_2]$.[11] The Ta–I bond length of 2.90 Å found for the 20% impurity of $[Ta(Me_3SiOCCOSiMe_3(dmpe)_2I]$ in **3** is 0.32 Å longer than the Ta–Cl distances in **2** and **3**, in excellent agreement with the known difference of 0.34 Å in Cl and I covalent radii.[25] Similar bond length variations occur in related seven-coordinate Mo and W complexes.[26] The Ta–O bond length of 2.293 (8) Å in the triflate analogue **4** is 0.28 Å shorter than the Ta–Cl distance in **2**, a difference also expected on the basis of the covalent radii[25] of oxygen (0.66 Å) and chlorine (0.99 Å).

The chelating dmpe groups in the equatorial plane are puckered and tipped in the direction of the axial (Y) ligands, halide or triflate, owing to steric interactions with the more bulky alkyne ligand. The metal therefore lies out of the mean plane through the four phosphorus atoms, by 0.441, 0.453, 0.449, and 0.274 Å, respectively, for compounds **1**–**4**. These values are consistent with the fact that the triflate ion is sterically more demanding than the chloride ion. Similar conclusions can be drawn from the dihedral angles (α) about the C–C bonds of dmpe chelate rings, which are less puckered (α = 25.4°, 32.4°, and 32.1°) for compounds **1**, **2**, and **3** than for compound **4** (α = 47.2° and 52.7°). The different steric demands of the chloride and triflate anions are further revealed by the dihedral angles between planes defined by P–M–P groups which are nearly identical for **1**, **2**, and **3** (26.0°, 27.1°, and 26.8°) and are smaller by about 10° in the case of **4** (17.2°) as a consequence of the greater steric bulk of triflate compared to chloride. All five-membered metal–dmpe chelate rings exhibit half-chair (C_2) conformations,[27] where the twofold axis passes through a phosphorus atom and the midpoint of the opposite bond, except for one of the rings in **4** ((Ta–P1–C13–C23–P2), where the twofold axis passes through the metal and the midpoint of the bond between the methylene carbon atoms.

The geometry of the coordinated bis(trimethylsiloxy)ethyne ligands in **1**–**4** is comparable to that of other four-electron-donating alkyne complexes of Ta (Table VI). These structural parameters have been used to characterize bound alkynes as four-electron vs. two-electron donors. As can be seen from Table VI, the bis(trimethylsiloxy)ethyne ligands of **1**–**4** fall into the four-electron donor category.[22,23] The geometry of the alkyne ligand also closely resembles that of the bis(dialkylamino)ethyne ligands formed from analogous reductive coupling of isocyanides. The M–C bond lengths of the coupled isocyanide ligands all lie in the range 2.026 (8) to 2.053 (4) Å, while the C–C bond lengths vary from 1.35 (2) to 1.402 (8) Å, and the C–C–N angles from 127.9 (3)° to 129.8 (8)°.[2,7]

Comparison of the molecular structures of **1**–**4** with those of **5** and **6**, the seven-coordinate niobium and tantalum starting materials, reveals that the coordination geometry of the metals undergoes subtle changes upon reductive coupling (Figure 3). The metal atoms of **1**–**4** are more displaced from the best planes through the P_4 atoms (toward the alkyne ligand, see above) than is the case for **5** and **6** (~0.36 Å), reflecting possibly the greater steric demands of the bulky $SiMe_3$ groups of the coupled complex. A more significant change in the Nb or Ta coordination sphere upon reductive coupling, however, is the orientation of the C–C vector. As shown in Figure 3, the C–M–C planes in **5** and **6** are staggered with respect to the M–P bond axes, resulting in nearly perfect C_{2v}-capped trigonal-prismatic geometry. In **1**–**4**, the C–C bonds are twisted by 45°, so that they are aligned parallel to one of the P–Ta–P vectors, making the D_{5h} pentagonal bipyramid the closest seven-coordinate idealized reference polyhedron.[26e] The pentagonal plane (Figure 3) is formed by C, C′, P1, P1′, and Cl (all deviations <0.05 Å); the apical ligands are P2 and P2′; and the P2–M–P2′ angle is 164.1 (1)°. Similarly distorted pentagonal-bipyrimidal geometry was seen in $[Ta(\eta^4\text{-naphthalene})(dmpe)_2Cl]$[24] and $[Ta(\eta^4\text{-anthracene})(dmpe)_2Cl]$.[11] Inspection of bond angles at the metal center confirms that the pentagonal bipyramid is the best seven-coordinate geometric assignment for **1**–**4**, with appreciable distortions from idealized pentagonal bipyramidal geometry being mainly due to the presence of three chelating ligands.

The eclipsed ligand conformation just described for **1**–**4** may be adopted in the solid state in order to place the bulky trimethylsilyl groups in the sterically least demanding position between the dmpe ligands. Electronic factors involving attainment of the best overlap of metal d and alkyne π^* orbitals may also be involved, however, as was found to be the case in the solid-state geometries of some other high-coordinate complexes with π-accepting ligands.[26f]

NMR and IR Spectral Properties. The NMR spectra of **2** are also consistent with the assignment of the bis(trimethylsiloxy)ethyne ligand as a four-electron donor. The ^1H, ^{13}C, and ^{31}P NMR chemical shifts are almost unchanged from those of **6**, the uncoupled starting mate-

Table VI. Geometry of Coordinated Alkynes in Various Complexes[a]

complex	C≡C, Å	M–C, Å	C–C–X, deg	ref
C_2Ph_2	1.198 (3)		178.2 (2)	*b*
two-electron donating alkynes				
$Cp_2Ti(CO)(C_2Ph_2)$	1.285 (10)	2.107 (7)	142.3 (7)	*c*
$Cp_2Mo(C_2Ph_2)$	1.269 (7)	2.144 (6)		*d*
$Cp(C_4Ph_4)Nb(CO)(C_2Ph_2)$	1.26 (3)	2.22 (2)	142 (4)	*e*
four-electron donating alkynes				
$[pyH][TaCl_4(py)(C_2Ph_2)]$	1.325 (12)	2.068 (8)	139.7 (8)	*f*
$Cp^*TaCl_2(C_2Ph_2)$	1.337 (8)	2.071 (6)	139.4 (9)	*g*
$[Nb(Me_3SiOCCOSiMe_3)(dmpe)_2Cl]$ (**1**)	1.310 (6)	2.074 (3)	133.4 (2)	*h*
$[Ta(Me_3SiOCCOSiMe_3)(dmpe)_2Cl]$ (**2**)	1.339 (9)	2.065 (5)	132.3 (3)	*h*
$[Ta(Me_3SiOCCOSiMe_3)(dmpe)_2Cl_{0.8}I_{0.2}]$ (**3**)	1.316 (9)	2.065 (4)	132.7 (2)	*h*
$[Ta(Me_3SiOCCOSiMe_3)(dmpe)_2(OSO_2CF_3)]$ (**4**)	1.36 (1)	2.07 (1)	134 (5)	*h*

[a] Numbers in parentheses are estimated standard deviations in the last digit(s) listed. [b] Mavridis, A.; Moustakali-Mauridis, I. *Acta Crystallogr., Sect. B: Struct. Crystallogr. Cryst. Chem.* **1977**, *B33*, 3612. [c] Fachinetti, G.; Floriani, C.; Marchetti, F.; Mellini, M. *J. Chem. Soc., Dalton Trans.* **1978**, 1398. [d] DeCian, A.; Colin, J.; Schappacher, M.; Ricard, L.; Weiss, R. *J. Am. Chem. Soc.* **1981**, *103*, 1850. [e] Pasynskii, A. A.; Skripkin, Y. V.; Eremenko, I. L.; Kallinnikov, V. T.; Aleksandrov, G. G.; Struchkov, Y. T. *J. Organomet. Chem.* **1979**, *165*, 39. [f] Cotton, F. A.; Hall, W. T. *Inorg. Chem.* **1980**, *19*, 2352. [g] Smith, G.; Schrock, R. R.; Churchill, M. C.; Youngs, W. J. *Inorg. Chem.* **1981**, *20*, 387. [h] This work.

(24) Albright, J. O.; Datta, S.; Dezube, B.; Kouba, J. K.; Marynick, D. S.; Wreford, S. S.; Foxman, B. M. *J. Am. Chem. Soc.* **1979**, *101*, 611.
(25) Pauling, L. In *The Nature of the Chemical Bond*, 3rd ed.; Cornell University Press: Ithaca, NY, 1960; p 224.
(26) (a) Lewis, D. F.; Lippard, S. J. *Inorg. Chem.* **1972**, *11*, 621. (b) Drew, M. G. B.; Wilkins, J. D. *J. Chem. Soc., Dalton Trans* **1973**, 2664. (c) Drew, M. G. B.; Wolters, A. P. *Acta Cryst.* **1977**, *33B*, 1027. (d) Lam, C. T.; Novotny, M.; Lewis, D. L.; Lippard, S. J. *Inorg. Chem.* **1978**, *17*, 2127. (e) Szalda, D. J.; Dewan, J. C.; Lippard, S. J. *Inorg. Chem.* **1981**, *20*, 3851. (f) Burgmayer, S. J. N.; Templeton, J. L. *Inorg. Chem.* **1985**, *24*, 2224. (g) Fong, L. K.; Fox, J. R.; Foxman, B. M.; Cooper, N. J. *Inorg. Chem.* **1986**, *25*, 1880.
(27) Eliel, E. L. In *Stereochemistry of Carbon Compounds*; McGraw-Hill: New York, 1962; Chapter 9.

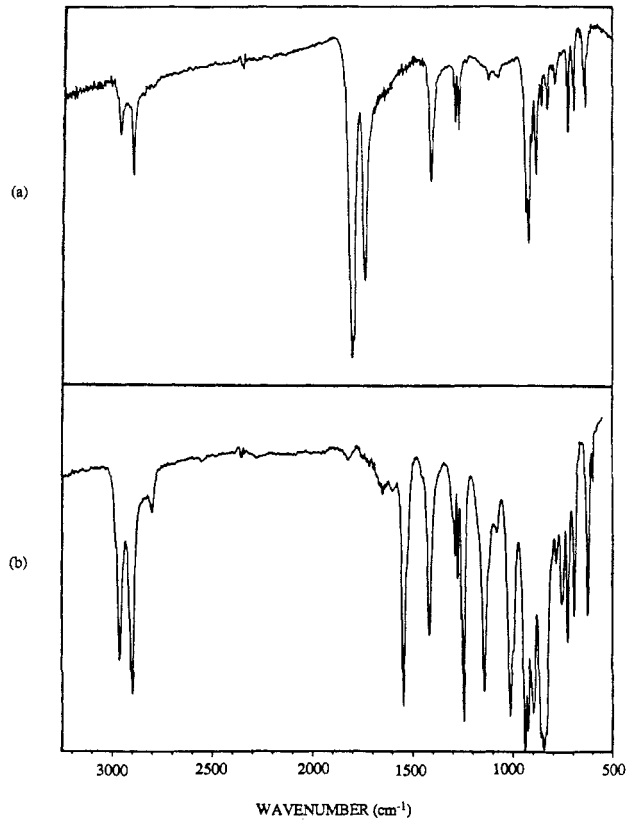

Figure 4. FTIR spectra of (a) $[Ta(dmpe)_2(CO)_2Cl]$ (**6**) and (b) $[Ta(Me_3SiOCCOSiMe_3)(dmpe)_2Cl]$ (**2**) in KBr pellets.

rial; the one large difference is in the position of the ^{13}C resonance of the coupled CO ligands. These resonances occur at 273 ppm for **6** and experience a 60 ppm upfield shift, to 212 ppm, for **2**. Also, a phosphorus–carbon coupling of 15 Hz is observed for the alkyne carbons of **2**, resulting in a quintet, while the CO carbons of **6** appear as a singlet in the ^{13}C NMR spectrum. The position of the ^{13}C resonance of the α-carbons of bound alkynes has been used to assign them as four-, three-, or two-electron donors.[22c,d] By this criterion, **2–4** are four-electron donors.

Both the structural and spectroscopic properties of the coupled ligands of **1–4** much more closely resemble those of the alkyne ligands derived from the reductive coupling of isocyanides[7] than those of any other ligand derived from reductive coupling of CO.[6] In the IR spectra of both the coupled CNR and CO complexes a new, medium-to-strong band, characteristic of the coupled ligand, appears. In the CNR case, this peak occurs between 1584 and 1687 cm^{-1}.[2,7] In the CO case, it falls ~1540 cm^{-1}, while the two strong terminal CO stretching bands in the starting compound **6** disappear (Figure 4). This 1540 cm^{-1} band is attributed to the C≡C (or C=O) stretches of the coupled ligand.

Only the tantalum compounds **2–4** were analyzed by ^{31}P NMR spectroscopy, since the large quadrupole moment associated with the niobium (^{93}Nb) nucleus causes severe broadening of the signals of **1**. The ^{31}P NMR spectrum of **2** consists of a singlet at 25.0 ppm, while in **4** the peak shifts to 27.8 ppm. In the iodide-capped impurity in **3**, the resonance occurs at 14.0 ppm. The equivalence of the four phosphorus sites is also revealed by their equivalent coupling to the alkyne carbon atoms. ^1H and ^{13}C NMR spectra also demonstrate that, in solution, **2–4** have effective C_{2v} symmetry. Only one resonance appears for the dmpe methylene carbon atoms, and the dmpe methyl carbon atoms form two distinct sets, those directed toward the capping ligand and those directed toward the alkyne, as is seen in **6** and other capped trigonal prismatic compounds containing the two equatorial chelating dmpe groups.[11,24] The NMR spectra do not distinguish between a fluxional geometry for solutions of **2–4** and a static one in which the alkyne ligand has rotated 45° from its position in the crystal (Figure 3), giving a capped trigonal prismatic structure having C_{2v} symmetry. The fluxional process that may best account for the solution NMR spectra of **2–4** is rotation of the alkyne ligand around the Ta–Cl vector. This process occurs in at least two other related seven-coordinate complexes, $[Mo(CN\text{-}t\text{-}Bu)_5(CNH\text{-}t\text{-}Bu)_2][BPh_4]_2$[11] and $[Ta(\eta^4\text{-naphthalene})(dmpe)_2Cl]$.[24]

^{31}P NMR spectra taken at various intervals during the reduction of **6** with Na(Hg) show four signals at 32.3, 22.4, 11.6, and 7.9 ppm during the initial stages of the reduction. Two of these disappear as the reaction proceeds, leaving the two at 22.4 and 7.9 ppm, which are known to be those of $[Ta(CO)_2(dmpe)_2]^-$.[20] Since addition of Me_3SiCl to this latter species generates **2**, ^{31}P NMR spectroscopy should prove to be useful in future mechanistic studies of eq 3.

Summary and Conclusions. The reductive coupling of two carbon monoxide ligands to form coordinated alkynes occurs in good yield for seven-coordinate $[Nb(CO)_2(dmpe)_2Cl]$ and $[Ta(CO)_2(dmpe)_2Cl]$ complexes. The resulting $[Nb(Me_3SiOCCOSiMe_3)(dmpe)_2Cl]$, $[Ta(Me_3SiOCCOSiMe_3)(dmpe)_2Cl]$, $[Ta(Me_3SiOCCOSiMe_3)(dmpe)_2I]$, and $[Ta(Me_3SiOCCOSiMe_3)(dmpe)_2(OTf)]$ compounds have been fully characterized structurally and spectroscopically. The 40% Na/Hg reductive coupling procedure described here is a significant improvement over the activated Mg route previously communicated,[10] requiring less expensive starting materials and simpler reaction conditions. Since addition of Me_3SiCl to *cis*-$[Ta(CO)_2(dmpe)_2]^-$, generated from $[Ta(CO)_2(dmpe)_2Cl]$ by reaction with 40% Na/Hg, yields $[Ta(Me_3SiOCCOSiMe_3)(dmpe)_2Cl]$, at least one mechanistic pathway for reductive coupling in this system proceeds through formation of this anion.

The reaction chemistry described here has many analogies with the reductive coupling of coordinated alkyl isocyanides.[2,7] Both reductive couplings occur in seven-coordinate d^4 metal complexes having trigonal prismatic geometries and close nonbonded contacts between the carbon atoms to be coupled. In both, the products are metal complexes having structures similar to those of their uncoupled precursors but in which a four-electron donating alkyne has replaced two neutral, two-electron donor ligands; in both, the newly formed alkynes are unknown in the free state, although analogous acetylene diethers have been synthesized.[28] Both reactions are quite general. In the isocyanide case, the metal of the substrate complex, its capping ligand, the supporting ligands, the reducing agent, and the isocyanide used can all be varied.[2,7] In the CO coupling, the metal of the substrate complex, the reducing agent, Lewis acid, and the silyl halide used similarly can be varied. This generality is an uncommon feature in other CO coupling systems. In fact, the only differences between the isocyanide and CO coupling reactions are ones of degree, stemming principally from the difference in bond strength of the C≡X moiety. The C≡O bond of carbon monoxide is much stronger (257 kcal/mol) than the C≡N bond of isocyanide (estimated to be less than the 184 kcal/mol value for C≡N),[29] and it is therefore more difficult to activate CO since the transition state involves weakening of the stronger C≡O bond. The steric, geometric, and electronic factors that were previously iden-

(28) Serratosa, F. *Acc. Chem. Res.* **1983**, *16*, 170.
(29) Weast, R. C. In *Handbook of Chemistry and Physics*; CRC Press: Boca Raton, FL, 1980; p F-221.

tified to promote C–C bond formation in the isocyanide systems therefore had to be applied to a greater degree in the CO case. A more electron-rich substrate complex was needed, closer nonbonded carbon–carbon contacts had to be developed, a stronger reducing agent and an R group (Me_3Si) preferential for oxygen were used, and Lewis acid activation to reduce the C≡O bond order was found to be necessary. That these factors favoring reductive coupling could be extrapolated from the isocyanide to the carbonyl case suggests that it might be possible to couple reductively other linear ligands, for example NO, carbenes, carbynes, CN^-, or acetylides.

Acknowledgment. This work was supported by National Science Foundation Grant NSF CHE85-42205.

Registry No. 1, 109467-49-4; 2, 99797-93-0; 4, 109467-51-8; 5, 66507-17-3; 6, 61916-36-7; $[Ta(Me_3SiOCCOSiMe_3)(dmpe)_2I]$, 109467-50-7; $[(C_5Me_5)_2ZrCl_2]$, 54039-38-2; $Me_3SiOSO_2CF_3$, 27607-77-8.

Supplementary Material Available: Tables S1–S8 containing non-hydrogen atom thermal parameters and hydrogen atom positional parameters for 1–4 (4 pages); listings of structure factors for 1–4 (47 pages). Ordering information is given on any current masthead page.

Ab Initio Calculations on Some C_3SiH_4 Isomers

George W. Schriver* and Mark J. Fink

Department of Chemistry, Tulane University, New Orleans, Louisiana 70118

Mark S. Gordon*

Department of Chemistry, North Dakota State University, Fargo, North Dakota 58105

Received February 27, 1987

Restricted Hartree–Fock ab initio calculations have been performed on various isomers of silacyclobutadiene (C_3SiH_4). Geometry optimizations were performed by using various basis sets. Geometric results were similar, but proper description of relative energies required the larger 6-31G* basis. Calculations treating election correlation at the MP2 level were performed on the seven lowest energy structures. These calculations gave similar results. The most stable species found is 2-methylsilacycloprop-2-en-1-ylidene. Silacyclobutadiene is almost 60 kcal mol^{-1} less stable, while silatetrahedrane lies a further 32 kcal mol^{-1} higher in energy. The most stable isomer with normal valence is 2-silabut-1-en-3-yne, 28.2 kcal mol^{-1} above the global energy minimum.

Introduction

There is currently much interest in the thermal isomerization of organosilicon molecules that are strained or possess an unsaturated silicon atom. The isomers of C_3SiH_4 are particularly relevant in this context, since many of them contain these structural features and the analogous hydrocarbons such as cyclobutadiene, methylenecyclopropene, and tetrahedrane have been the object of many investigations. The experimental work of one of us involves the photochemical generation of cyclopropenylsilylenes (substituted derivatives of a C_3SiH_4 isomer) and their subsequent transformations. In connection with this work, ab initio molecular orbital calculations have been performed on a number of isomers of the parent, C_3SiH_4, system. Species studied include the parent cyclopropenylsilylene, **1**, silacyclobutadiene, **2**, silatetrahedrane, **3**, silylidenecyclopropene, **4**, 2-silabicyclo[1.1.0]butanylidene, **5**, 2-methyl-1-silacycloprop-2-en-1-ylidene, **6**, 2-methylenesilacycloprop-1-ylidene, **7**, silacyclobut-2-en-1-ylidene, **8**, and 1- and 2-silamethylenecyclopropene, **9** and **10**. For comparison, eight isomeric acyclic silenes and silylenes were studied: 1- and 2-propynylsilylene, **11** and **12**, methylethynylsilylene, **13**, 1-sila-1-buta-1,3-dienyldiene, **14**, 1,2-propadienylsilylene, **15**, 1-silabutatriene, **16**, and 1- and 2-silabut-1-en-3-yne, **17** and **18**. Calculations on several other isomers showed them to be higher in energy; they are not reported here. Our primary intent was to discover the energetic global minimum of the system and to determine how destabilized the other isomers were in relation to it. We were particularly interested in the relative stabilities of **1** and some of its possible isomerization products, such as **2**, **3**, **4**, and **5**.

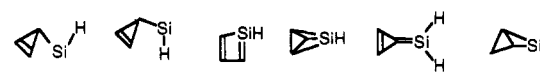

1a 1b 2 3 4 5

The relative stabilities of the isomers will be governed by various principles. First, the weakness of π bonding involving silicon should disfavor structures with silicon–carbon double bonds and especially those with silicon–carbon triple bonds. Where possible, alkyl substitution on silicon provides more stabilization than hydrogen substitution. The stability of silylenes (divalent silicon species) compared to tetravalent silicon is greater than that of carbenes compared with tetravalent carbon.[2] Finally, silacyclobutadiene may be somewhat destabilized due to antiaromaticity. Due to the poor π overlap noted above, this effect is liable to be small.

Several theoretical studies have been performed on silaethylene and its isomer, methylsilylene. Schaefer and co-workers[5] examined these compounds, along with silylmethylene, in both the singlet and triplet states. This study found silaethylene and methylsilylene to be close in energy, while the carbene isomers and all of the triplet

(1) Gordon, M. S. *Chem. Phys. Lett.* **1980**, *76*, 163–168.
(2) Walsh, R. *Acc. Chem. Res.* **1981**, *14*, 246–252.
(3) Gordon, M. S. *Chem. Phys. Lett.* **1978**, *54*, 9–13.
(4) Hood, D. M.; Schaefer, H. F., III *J. Chem. Phys.* **1978**, *68*, 2985–2986.
(5) Goddard, J. D.; Yoshioka, Y.; Schaefer, H. F., III *J. Am. Chem. Soc.* **1980**, *102*, 7644–7650.

0276-7333/87/2306-1977$01.50/0